Photodissociation of the Fluorene Cation: A Fourier Transform Ion Cyclotron Resonance Mass Spectrometric Study

Mark J. Dibben, David Kage, Jan Szczepanski, John R. Eyler,* and Martin Vala*

Department of Chemistry and Center for Chemical Physics, University of Florida, P.O. Box 117200, Gainesville, Florida 32611-7200

Received: January 7, 2001; In Final Form: April 3, 2001

The photodecomposition of the vapor phase fluorene cation has been studied using Fourier transform ion cyclotron resonance (ICR) mass spectrometry. Broad-band visible and ultraviolet irradiation for relatively short times (∼0.5 s) is shown to lead predominantly to sequential hydrogen atom loss, with one to five hydrogens lost. A relatively minor decomposition route for several precursor ions is the loss of H_2 (or 2H atoms). Longer irradiation times lead to various products resulting from multiple C−C bond cleavages. The "action" spectrum for the *m*/*z* 166 → 165 process reveals two major electronic absorption bands which correlate well with a previous matrix absorption spectrum of the parent ion. The $C_{13}H^+_{10-n}$ ($n = 0-5$) species have been isolated in the ICR mass spectrometer, irradiated further, and their photodecomposition followed kinetically. Solution of the appropriate coupled differential equations that govern the kinetics has enabled fits to the experimental data. Rate constants and branching ratios for the photodecomposition of fluorene and its dehydrogenated partner ions have been determined. The photoproduct ions observed suggest rapid isomerization in some excited states with ring openings playing a possible role in certain decomposition pathways.

I. Introduction

Polycyclic aromatic hydrocarbons (PAHs) have been proposed[1,2] as the species responsible for the so-called "unidentified interstellar infrared"(UIR) emission bands,[3] a series of bands now observed from a wide variety of objects in space. The most prominent of these bands appear at 3.3, 6.2, 7.8, 8.6, and 11.3 μm. Shortly after the original proposal that neutral and ionized PAHs might be responsible for the UIRs, it was suggested that dehydrogenated PAHs might also contribute to the nearly ubiquitous UIR bands.[4−12] This suggestion was an attempt to rationalize the discrepancy between the intensity distributions of the observed UIR bands and laboratory infrared absorption bands of neutral PAHs. This proposal has since proven unnecessary because of the discovery that the intensity distributions of ionized PAHs more closely mimic the UIR distribution than do those of the neutral PAHs. However, the idea still retains merit because of the high photon fluxes emitted from various stellar sources that could lead to PAH dehydrogenation and even greater fragmentation.

Allamandola and co-workers have pointed out that the PAHs can be expected to be extensively cycled throughout their lives.[13] Possibly originating in asymptotic giant branch (AGB) stars, the PAHs and other ejecta will be exposed to relatively cool photon sources, but in the course of their travels, the PAHs may also come into the vicinity of planetary nebula where they will be harshly irradiated by extremely hot stellar cores. Only those PAHs able to withstand these different radiation fields can be expected to survive in the long term. Leach and co-workers have remarked[14] that the existence of a limited number of PAHs is consistent with the requirements of the interstellar carbon budget, as recently revised by Snow and Witt.[15]

It is thus important to study the photodissociation products and pathways of the PAHs to understand the critical factors leading to PAH or PAH fragment structures which will retain stability over periods long on an astrophysical time scale. There have been a number of important previous studies on this topic. Cooks and co-workers used a variety of techniques including photodissociation to probe the unusual mass spectrometric decomposition behavior of PAHs and concluded that rearrangement of the carbon frameworks was probable after excitation and just prior to fragmentation.[16] Leger, Boissel, Desert, and d'Hendecourt presented a model calculation of the "photo-thermo-dissociation" process, in which energy absorbed from a UV photon is transferred to a molecule's internal vibrations and thence induces the ejection of a hydrogen or carbon fragment.[17] Boissel and co-workers showed that PAH cations held in an ion trap could be photodissociated (and lose hydrogens or acetylenes) after the absorption of several low energy photons.[18] A theoretical model involving sequential multiphoton absorption was later proposed to explain their results.[19] Allain, Leach, and Sedlmayr developed a model for the photodestruction of PAHs in the interstellar medium and concluded that to survive the different radiation fields the PAH had to contain 50 or more carbons.[20] The photoionization and photofragmentation processes in naphthalene and azulene cations were thoroughly studied by Leach and co-workers.[21] Jochims, Baumgartel, and Leach extended earlier work on the photostability of PAHs to include irregularly shaped PAHs, methyl-substituted PAHs, and related compounds and devised a photostability index, a measure of the propensity for hydrogen loss in PAH cations.[14] Lifshitz and co-workers have reported numerous studies of PAHs using time-resolved photoionization mass spectrometry.[22] Dunbar et al. have published a series of studies on the time-resolved photodissociation (TRPD) mass spectrometry (MS) of PAH ions.[23] An elegant study by Dunbar and co-workers on the TRPD/MS of naphthalene cation and its infrared radiative cooling showed that this approach may be used as an independent confirmation of absolute infrared intensities obtained from matrix studies or theoretical calculations.[24] Guo, Sievers, and Grutzmacher used the SORI -CID

10.1021/jp0100708 CCC: $20.00
Published on Web 06/06/2001

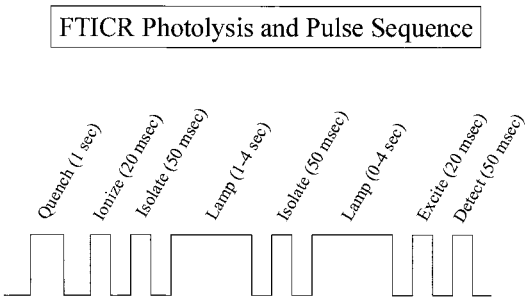

Figure 1. Typical FTICR timing pulse sequence used for experiments reported in this article.

(sustained off-resonance irradiation collision induced dissociation) method[25] to study sequential hydrogen loss from a series of PAHs.[26] Structural rearrangements were invoked to explain their results. Theoretical work on the probable stable fragments after acetylene loss from photoexcited naphthalene, anthracene, and phenanthrene cations has been reported by Granucci et al.[27] and Ling et al.[28] Schwartz and co-workers, using a combination of mass-spectrometric experiments, found that the loss of acetylene upon dissociative ionization of naphthalene did not lead to phenylacetylene, but probably to benzocyclobutadiene,[29] as predicted by Ling et al.[28] Other acyclic structures could not be excluded and are still possibilities. Joblin and co-workers laser-ablated pyrolyzed coronene into a Fourier transform ion cyclotron resonance mass spectrometer (FTICR/MS) and found evidence for larger, highly dehydrogenated oligimer species.[30] Ekern and co-workers reported the complete dehydrogenation of coronene ($C_{24}H_{12}^+$) and naphthopyrene ($C_{24}H_{14}^+$) using FTICR/MS with brief (500 ms) UV/visible photolysis exposures.[31] In a later report, these workers investigated a wide variety of PAH cations using FTICR and found evidence for dehydrogenation and fragmentation using broadband photoexcitation.[32] In the present paper, we focus on the fluorene cation and study its photodecomposition products and pathways.

II. Experimental Procedures

All experiments were performed on a home-built 2 T FT-ICR mass spectrometer.[33] Pulse sequencing and data collection is controlled by a newly acquired modular ICR data acquisition system (MIDAS),[34] developed in the National High Field FTICR Facility at the National High Magnetic Field Laboratory (NHMFL) in Tallahassee, FL. An ISA-MXI bus interface connects a PC to a five-slot VXI chassis. Pulse timing is initiated in a digital pattern generator (DG600VXI, Interface Technology) and expansion card (DG605VXI), both of which are interfaced to an instrument control module (ICM) that controls four 12-bit DC voltage outputs, four 8-bit DC voltage outputs, and 16 TTL triggers. The electron gun is also under the control of the ICM. An arbitrary waveform generator (Tektronix VX4790A) is used to generate the excitation waveforms. Up to 16 unique waveforms may be used in a single experiment. The waveforms are amplified via an RF power amplifier (ENI 2100L M2). A digitizer (Hewlett-Packard E1437A) collects the time domain signals generated by excited ions after amplification.

A typical timing pulse sequence is shown in Figure 1. Following a quench pulse to clear the cell of ions from previous experiments, the sample was ionized by electron impact. To minimize fragmentation, the voltage was set as low as possible (~14 eV) while still ensuring adequate ion formation. The *m*/*z* 166 fluorene parent ion was isolated using stored waveform inverse fourier transform (SWIFT)[35] waveforms to remove unwanted electron impact-formed fragments and ^{13}C isotope-containing ions. Ions were irradiated by a Xe arc lamp for one to four seconds and then either isolated for further irradiation or excited and detected using standard chirp pulses.

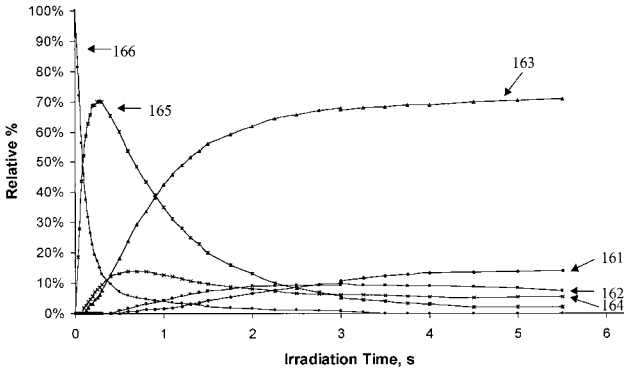

Figure 2. Relative abundance of the fluorene parent cation (*m*/*z* 166) and five dehydrogenated products (*m*/*z* 161−165) as a function of Xe lamp irradiation time.

The PAH sample (Aldrich) was inlet to the system through a leak valve (Varian, model 951-5100). Operating pressures, obtained with a 700 L/s diffusion pump (Alcatel), were typically 4×10^{-8} Torr. Ions were trapped in an open cylindrical cell 4.5 in. long with a 2.7 in. diameter.

The excitation source used in these studies was a broad band 300 W Xe arc lamp (ILC Technology, model LX300UV) with continuous output between 250 and 1100 nm (1.1−5 eV). The lamp was focused by a fused silica lens and illuminated the ions through a window in the end of the ICR vacuum chamber. An electronically operated shutter (Vincent Associates, Uniblitz VS35S2ZM1R1), controlled by a TTL signal from the data station, was used to control the length of the irradiation pulses.

Photodissociation "action" spectra were recorded using a small, fast monochromator (Farrand, 0.25 m). The excitation wavelength was scanned while monitoring the mass of the product ion ($[M-H]^+$) in the FTICR mass spectrometer.

III. Results

A. Hydrogen Loss. Previous work has shown that when irradiated for brief periods (500 ms), the fluorene cation loses up to five hydrogens.[32] Information on the mechanism of this loss was not reported, however. Some of the questions which remain include: (i) Are the hydrogens lost sequentially or simultaneously? (ii) Are they lost as atoms or molecules? (iii) From which positions are the hydrogens stripped? (iv) Does further fragmentation of fluorene occur with longer irradiation times? (v) If so, what are the primary decomposition routes and their yields and rates? (vi) And, what are the product ions and their structures? These questions are addressed here and in a subsequent paper.[36]

Figure 2 plots the time-dependence of the photolysis of the parent ion and its five dehydrogenated products. Irradiation was effected with the broad-band output of the Xe lamp. Shortly after commencement of irradiation, the *m*/*z* 166 parent decreases precipitously, while the *m*/*z* 165 product grows rapidly and is the dominant species after ca. 200 ms. After 1.5 s of photolysis, the *m*/*z* 163 product increases substantially and becomes the predominant product. Fragments at *m*/*z* 161, 162, 164, and 165 are also visible at longer times but never rise above ca. 15% abundance.

Although the intensity vs time plots in Figure 2 suggest sequential hydrogen loss, this possibility was probed further as follows. After ionization, each of the fragment peaks was isolated in turn, and irradiated briefly (~1 s). (Brief photolysis

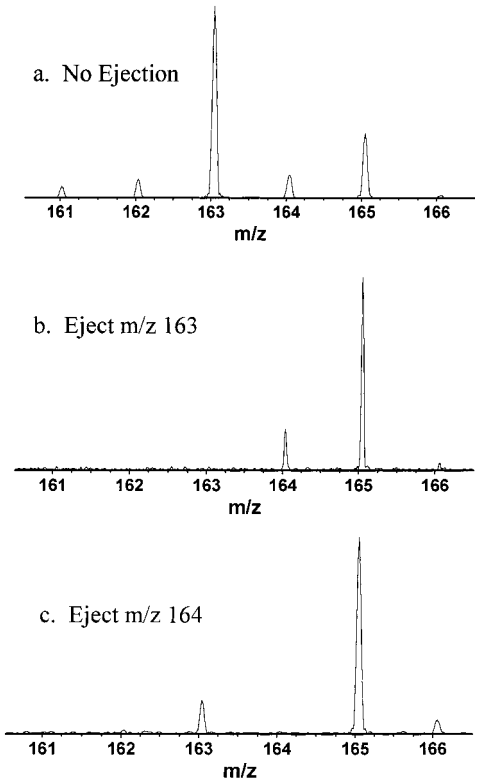

Figure 3. (a) FTICR spectrum (*m*/*z* 160−166 range) taken after Xe lamp irradiation (4 s) with no ejections. (b) FTICR spectrum (*m*/*z* 160−166 range) taken after Xe lamp irradiation (4 s) with the *m*/*z* 163 ion simultaneously ejected (using single frequency ejection, (SFE)). Note the absence of *m*/*z* 161 and 162 peaks, signifying sequential loss of hydrogen atoms. (c) FTICR spectrum (*m*/*z* 160−166 range) taken after Xe lamp irradiation (4 s), with the *m*/*z* 164 ion simultaneously ejected (with SFE). Note the presence of the *m*/*z* 163 peak, indicating the loss of 2 Hs (or H_2) from the *m*/*z* 165 ion.

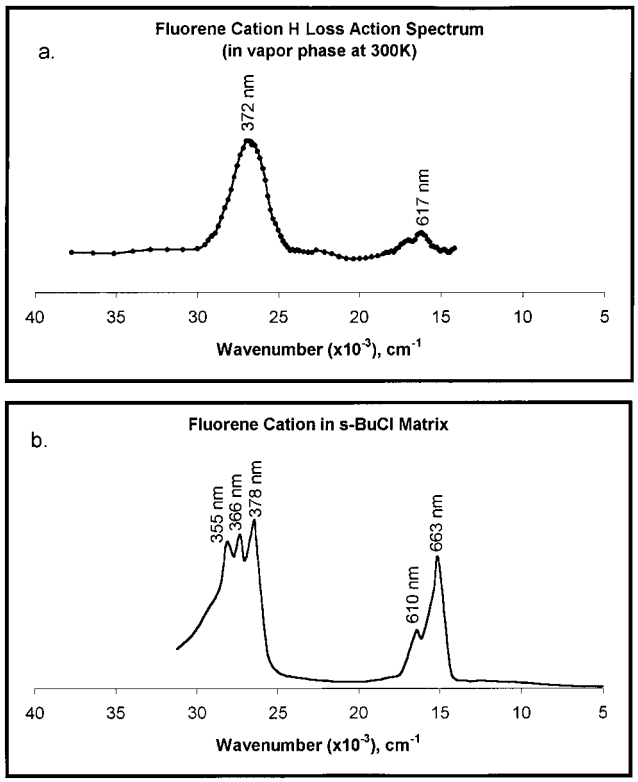

Figure 4. (a) "Action" spectrum obtained by monitoring the *m*/*z* 165 ion mass peak and scanning the wavelength with a monochromator/Xe lamp combination. (b) Absorption spectrum of the fluorene cation in a *sec*-butyl chloride solid matrix at 77 K. Adapted from ref 37.

times were essential since longer times resulted in the development of one or more lower mass peak(s), i.e., loss of two or more hydrogen atoms.) The next lower *m*/*z* mass peak is formed in all cases, showing conclusively that the primary dehydrogenation channel is sequential loss of single hydrogen atoms. It follows that, if a particular dehydrogenated product is ejected from the ICR cell, its successor, one amu lower, should then be absent. Comparison of Figures 3a and 3b shows this to be the case: when the *m*/*z* 163 product is ejected, no *m*/*z* 162 or 161 successor products are observed. A similar result was seen for ejection of all four species (*m*/*z* 162−166).

Loss of H_2 (or 2 H atoms) was also observed for two of the dehydrogenated precursors. For the *m*/*z* 165 species, losing only single H atoms (to form *m*/*z* 164 products), no *m*/*z* 163 (or lower) peaks would be observed, but as Figure 3c shows, the *m*/*z* 163 peak is clearly visible, indicating that the *m*/*z* 165 successor ion is capable of losing two hydrogens simultaneously (as H_2 or 2H) to produce *m*/*z* 163. Single frequency ejection of each of the *m*/*z* 162−165 species in turn revealed that only the *m*/*z* 163 and 165 species lose two hydrogens simultaneously. The branching ratio for *m*/*z* 165 dehydrogenation is ∼13% dual H loss and 87% single H loss, while for the *m*/*z* 163 dehydrogenation it is ∼34% dual hydrogen loss and 66% single hydrogen loss (vide infra). The even species (*m*/*z* 162, 164, and 166) only lose single hydrogens.

B. Wavelength Dependence. The wavelength dependence of dehydrogenation was also investigated. A small, fast monochromator was used to vary the irradiation wavelength while monitoring the mass abundance of a dehydrogenated product ion. While it would have been informative to record the "action" spectra of all the dehydrogenated product ions, the loss of sensitivity, resulting from the decrease in excitation flux upon insertion of the monochromator, precluded this and restricted us to only the *m*/*z* 166 → *m*/*z* 165 process.

Figure 4a shows the action spectrum for the loss of the first hydrogen from the fluorene cation. A broad peak is seen at ca. 617 nm along with another, more intense peak at 372 nm. This spectrum mimics reasonably well (cf. Figure 4b) the electronic absorption spectrum in a rigid matrix reported previously by Shida.[37] It can thus be concluded that excitation into either electronic state leads to dehydrogenation.

A full understanding of the dehydrogenation mechanism requires a discussion of the irradiation flux dependence for this process. The power output of the Xe lamp used is ∼0.05 W/nm in the 300−800 nm range yielding a photon flux of $\sim 6 \times 10^{15}$ photons s^{-1} cm^{-2} nm^{-1} at 372 nm. Neutral density filters were used to compare the amount of dehydrogenation of the full lamp output with that observed through the monochromator. Equivalent amounts were observed at 0.5% transmittance, which leads to an estimate of the photon flux as 3×10^{13} photons s^{-1} cm^{-2} nm^{-1} at 372 nm.

C. Further Fragmentation. Longer irradiation times (> ca. 1.5 s) lead to other photofragments with smaller *m*/*z* values. Figure 5 shows the spectrum of the lower mass products in the *m*/*z* 50−150 range. Major products appear at *m*/*z* 63, 87, 89, 108−111, 115, 132, and 139.

The precursors of these product ions were determined using the following irradiation−isolation−ejection sequences. After ionization, the cell contents were irradiated for a fixed time, and the *m*/*z* 161−165 ions were isolated, each in turn. The isolated ion was subjected to further photolysis and its abundance followed as a function of irradiation time. During this

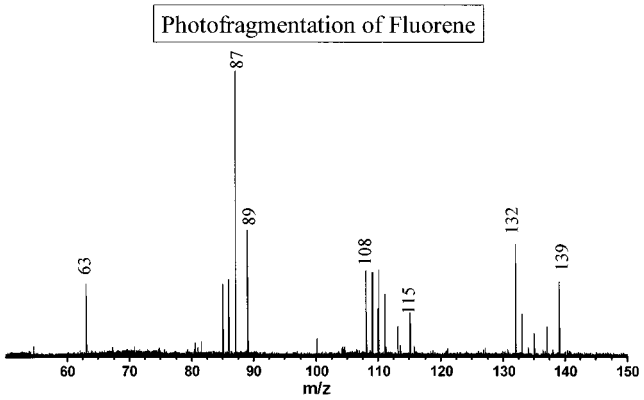

Figure 5. FTICR spectrum (*m/z* 50−150 range) after Xe lamp irradiation (1.5 s) and no ejections or isolations.

TABLE 1: Fragment Ion Yields and Rate Constants for Photodissociation of the Fluorene Cation ($C_{13}H_{10}^+$) and Its Dehydrogenated Products ($C_{13}H_{10-n}^+$ $n = 1-5$)

precursor ion	precursor ion (*m/z*)	fragment ion	fragment ion (*m/z*)	percent yield (%)	rate constant *i*	rate constant k_i ($\times 10^1\ s^{-1}$)[a,b]
$C_{13}H_{10}^+$	166	$C_{13}H_9^+$	165	92.2	1	32.2
		$C_{11}H_8^+$	140	2.0	2	0.71
		$C_{11}H_7^+$	139	1.6	3	0.57
		$C_9H_8^+$	116	1.6	4	0.57
		$C_9H_7^+$	115	2.1	5	0.74
		$C_7H_5^+$	89	0.4	6	0.13
$C_{13}H_9^+$	165	$C_{13}H_8^+$	164	42	8	5.5
		$C_{13}H_7^+$	163	2	7	0.3
		$C_{11}H_7^+$	139	25	10	3.3
		$C_9H_7^+$	115	31	9	4.2
$C_{13}H_8^+$	164	$C_{13}H_7^+$	163	100	19	27
$C_{13}H_7^+$	163	$C_{13}H_6^+$	162	50	21	0.51
		$C_{13}H_5^+$	161	22	20	0.23
		$C_7H_5^+$	89	17	15	0.18
		$C_7H_3^+$	87	11	22	0.11
$C_{13}H_6^+$	162	$C_{13}H_5^+$	161	100	23	19.2
$C_{13}H_5^+$	161	$C_{11}H_3^+$	135	22	24	0.26
		$C_9H_3^+$	111	4	27	0.05
		$C_7H_3^+$	87	53	25	0.62
		$C_5H_3^+$	63	21	26	0.25

[a] Rate constants valid for the photon fluxes used in this study. [b] Rate constants are for processes shown in Figure 6.

procedure, the other *m/z* 16× peaks were ejected. The first photolysis created a detectable population of the *m/z* 161−165 ions. The buildup of photoproducts was scrutinized during the second irradiation. The first photolysis step was omitted for the *m/z* 166 ion since a large population of the parent ion was already present due to the ionization process.

Table 1 gives the main photodecomposition products for fluorene and its dehydrogenated partners, while Figure 6 gives a visual overview of the fragmentation pathways. The fragmentation pathways followed by the parent and each dehydrogenated product contain clues to the structures of their precursors. They will be discussed in a future paper. The fragments observed from the parent and its dehydrogenated successor ions are discussed in turn below.

m/z 166: The *m/z* 166 parent ion decomposes predominantly to the *m/z* 165 ion, with a 92% yield. Other primary fragments are: *m/z* 140 ($C_{11}H_8^+$) and 139 ($C_{11}H_7^+$), 116 ($C_9H_8^+$) and 115 ($C_9H_7^+$), and 89 ($C_7H_5^+$). Secondary products appear from some, but not all, of these primary fragments. For example, *m/z* 139 photolyzes to give both *m/z* 89 ($C_7H_5^+$) and 87 ($C_7H_3^+$), while *m/z* 115 ($C_9H_7^+$) yields *m/z* 89 ($C_7H_5^+$) and 63 ($C_5H_3^+$) but not

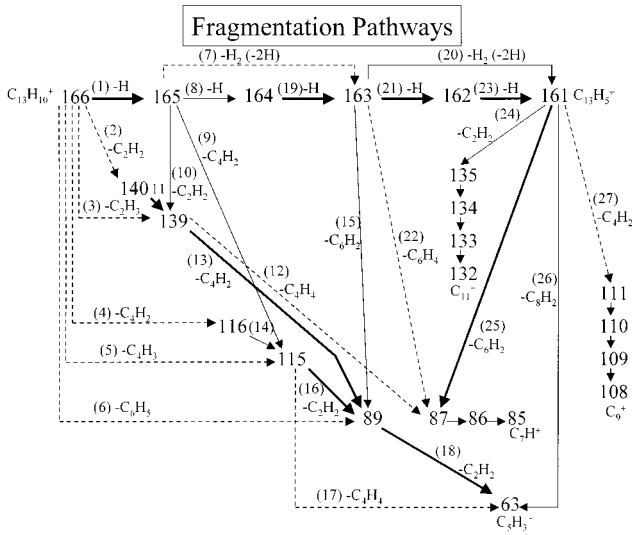

Figure 6. Photodecomposition pathways and products from the *m/z* 166 fluorene parent ion. Bold lines indicate yields of 50% or greater, thin lines indicate yields between 15 and 49%, and dashed lines indicate yields less than 15%.

m/z 87 ($C_7H_3^+$). The *m/z* 87 ($C_7H_3^+$) species is found to dehydrogenate sequentially to *m/z* 85 (C_7H^+).

m/z 165: The decomposition of the *m/z* 165 product leads to *m/z* 164 ($C_{13}H_8^+$), 163 ($C_{13}H_7^+$), 139 ($C_{11}H_7^+$), and 115 ($C_9H_7^+$). The *m/z* 139 ion decays to *m/z* 89 ($C_7H_5^+$) and 87 ($C_7H_3^+$), while the *m/z* 115 ion decays to *m/z* 89 ($C_7H_5^+$) and *m/z* 63 ($C_5H_3^+$).

m/z 164: This ionic species loses only one hydrogen.

m/z 163: The photofragmentation of this species leads to *m/z* 89 ($C_7H_5^+$) and 87 ($C_7H_3^+$) products, as well as to further dehydrogenation to give *m/z* 162 and 161.

m/z 162: This species only loses one hydrogen.

m/z 161: For the *m/z* 161 ion ($C_{13}H_5^+$), fragments containing more than 5 hydrogen atoms are not possible. As Table 1 indicates the major fragment peaks are *m/z* 63 ($C_5H_3^+$), *m/z* 87 ($C_7H_3^+$), *m/z* 135 ($C_{11}H_3^+$), and *m/z* 111 ($C_9H_3^+$). Figure 6 shows that hydrogens may be stripped sequentially from the latter three species. The *m/z* 135 ion may go to *m/z* 132 (C_{11}^+), while the *m/z* 111 and the *m/z* 87 products form the *m/z* 108 (C_9^+) and *m/z* 85 (C_7H^+) species, respectively.

D. Kinetics. The branching ratios and rate constants for photodecomposition of the fluorene cation and its dehydrogenated partners were determined. The ion peak heights vs. time plots were fit by solving the appropriate set of coupled differential equations. For short irradiation times, only dehydrogenation products were present and their rate constants were readily determined. For longer irradiation times, the abundance of other photoproducts grew in importance. By fixing the previously determined rate constants for the dehydrogenated product ions, the remaining rate constants were determined simultaneously using a program called KINFIT[38] which numerically solved the equations and fit the experimental curves. The rate constants (k_i) and percent yields obtained are given in Table 1.

Several interesting observations are evident from the table. First, the primary photodecomposition route for the *m/z* 166 parent ion is single H atom loss with a greater than 90% yield. The yields from the other five routes are each 2% or less. Second, the rates of dehydrogenation of the even mass species (*m/z* 166, 164, 162) are faster (5 to 10 times) than the decomposition of the odd mass species. Third, the bottleneck

in the sequential dehydrogenation from the *m*/*z* 166 to *m*/*z* 161 species is the *m*/*z* 163 → *m*/*z* 162 step, which is ∼10 times slower (0.051 s^{-1}) than its closest competitor (*m*/*z* 165→ *m*/*z* 164, 0.55 s^{-1}). Fourth, the odd mass species (*m*/*z* 165, 163, 161) are more prone to lose larger neutral fragments (i.e., larger than hydrogen) as compared with the even mass species. For example, the *m*/*z* 165 ion decomposes ∼40% to *m*/*z* 164, ∼30% to *m*/*z* 115, and ∼25% to *m*/*z* 139, all comparable percentages, while the *m*/*z* 162 and 164 precursor ions decompose 100% via single H atom loss.

IV. Discussion

Detailed studies of the photodecomposition of vapor phase fluorene cation are reported in this paper. Both dehydrogenation and further fragmentation is shown to occur with broad band UV/visible irradiation. In the original report on fluorene ion photolysis,[32] it was stated that between one and five hydrogens were lost with no other products observed. Although this observation appears to contradict the present results, it becomes understandable on closer analysis. The primary decomposition route, i.e., the one possessing the largest rate constants, is sequential H atom loss. The appearance of a large *m*/*z* 163 peak results from its further slow decomposition. A detectable quantity of smaller fragmentation products requires longer irradiation times. The original exploratory experiments[31,32] irradiated the ions for periods of only 500 ms, clearly insufficient to produce the lower mass fragments observed here.

The loss of the hydrogens from the fluorene cation as well as the further decomposition probably occurs via a multiple-photon excitation process. Boissel and co-workers have outlined[18,19] a possible mechanism that involves the sequential absorption of visible and UV photons that increases the internal energy of the precursor ion stepwise until the dissociation limit is reached. This mechanism relies heavily on rapid electronic relaxation and intramolecular vibrational redistribution (IVR)[39] rates. The latter rates are known[40] to occur on the subnanosecond time scale in large molecules, such as the PAHs, and are therefore many orders of magnitude higher than the expected dissociation rates. With sufficiently high absorption rates, multiple photons can be expected to pump the molecule above its fragmentation threshold.

The geometries of the precursor ions and their subsequent products are also of great interest. In an important study, Pachuta et al. suggested that the similarity between the fragment ions and the neutral products formed from a number of different PAHs probably results from rapid isomerization leading to several common intermediate structures.[16] Whether the dehydrogenated fluorene product ions retain their original carbon framework or rearrange to isomers is an open question. There is theoretical evidence that the sequential H atom loss occurs first from the sp^3-carbon and then exclusively from one of the two six-membered rings.[36] This would create a radical with four unpaired electrons, one on each of four adjacent carbons. Subsequent bond closures to form two triple bonds in one ring (i.e., a di-yne) is unlikely because of ring strain. Ring opening via a retro-Bergman cyclicization has been proposed by Sun, Grutzmacher, and Lifshitz for a similar photodecomposition in perchlorofluorene, $C_{13}Cl_{10}^+$.[41] These workers propose that one ring opens in the $C_{13}Cl_7^+$ species, which then loses two chlorines. Finally, the other ring opens to form monocyclic $C_{13}Cl_5^+$. We propose an alternate scheme below.

Fragmentation of the *m*/*z* 166 parent species leads to *m*/*z* 89 ($C_7H_5^+$), 115 ($C_9H_7^+$), 116 ($C_9H_8^+$), 139 ($C_{11}H_7^+$), 140 ($C_{11}H_8^+$), and 165 ($C_{13}H_{12}^+$) species. From a knowledge of the products formed, it is tempting to speculate on the possible structural rearrangements that may occur after photoexcitation. One such structure is the monocyclic ring formed by the cleavage of the C−C bonds between the two six-membered rings and the central five-membered ring. Precedence for this suggestion comes from theoretical work on fluorene's cousin, biphenylene, by Beck et al. These workers concluded that electronic excitation of biphenylene, with its two six-membered rings joined by a four-membered ring, leads to a structure that resembles a (12)-annulene ring with two transannular interactions.[42] This is structurally similar to the monocyclic ring structure proposed here for fluorene cation. Extraction of a neutral acetylene (C_2H_2) would then leave a chainlike $C_{11}H_8^+$ (*m*/*z* 140) species (cf. fragmentation b in Figure 7). Simultaneous loss of one of the hydrogens on the sp^3 carbon and an acetylene would give the $C_{11}H_7^+$ (*m*/*z* 139) species (fragmentation c). Stripping of a neutral C_4H_2 fragment yields the $C_9H_8^+$ (*m*/*z* 116) species (fragmentation d), while simultaneous loss of C_4H_2 and H would produce the observed $C_9H_7^+$ (*m*/*z* 115) product ion. Finally, simultaneous loss of a hydrogen and a C_6H_4 neutral fragment would give the minor $C_7H_5^+$(*m*/*z* 89) species (fragmentation e).

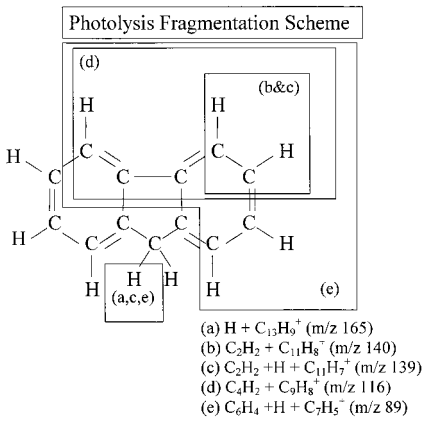

Figure 7. Possible photofragmentation scheme of the *m*/*z* 166 fluorene parent ion.

The decomposition of the *m*/*z* 165 ($C_{13}H_{12}^+$) ion also follows simply from the proposed monocyclic ring intermediate. After the first hydrogen is stripped from the sp^3 carbon to yield this precursor (fragmentation a in Figure 7), loss of C_2H_2 and C_4H_2 neutral fragments would then produce the observed $C_{11}H_7^+$ (*m*/*z* 139) and $C_9H_7^+$ (*m*/*z* 115) products, respectively. The *m*/*z* 89 product yield is presumably too small to be observed.

Rapid dehydrogenation leads mainly to the *m*/*z* 164, 163, 162, and 161 species. Structures for these precursors may involve different kinds of rearrangements and different isomeric structures. Discussion of these possibilities is left for a future paper.[36]

V. Conclusions

By a combination of isolations and ejections in the ICR cell, it is established that the H atom loss from fluorene is sequential with a loss of up to five H atoms. Only the odd mass species, *m*/*z* 163 and 165, may also lose two hydrogens simultaneously (as 2H or H_2). The even mass species *m*/*z* 162, 164, and 166 lose only single hydrogen atoms. The action spectrum of the *m*/*z* 166 → *m*/*z* 165 decomposition mimics closely the matrix spectrum of the fluorene cation reported by Shida previously.

Irradiation times longer than 2s lead to photofragments with smaller masses. Products appear at *m*/*z* 63, 87, 89, 111, 115, 116, 135, 139, and 140, plus the dehydrogenated species at *m*/*z* 161−165. By isolating the parent and dehydrogenated precursor

partners in turn and irradiating them further, the photoproducts originating from each have been found.

Rate constants and branching ratios for each of these decomposition pathways have been determined. Kinetic plots (mass abundance vs irradiation time) for each precursor and its products were fit by computer solution of a series of coupled differential equations. Sequential single H atom loss is shown to be the preferred decomposition pathway. Isomerization of the fluorene cation to a monocyclic ring structure is postulated to precede the decomposition to the observed lower mass products.

Acknowledgment. The authors acknowledge the National Aeronautics and Space Administration and the Petroleum Research Foundation, administered by the American Chemical Society, for their support of this research, and the Northeast Regional Data Center for a grant under the Research Computing Initiative for the computer time. Acquisition of the data system was made possible with funding from the University of Florida College of Liberal Arts and Sciences. We thank the National High Field FTICR Facility at the NHMFL for constructing the instrument control module and electron ionization controller, and Gordon Anderson at the Pacific Northwest National Laboratories for providing the low-noise preamplifier.

References and Notes

(1) Leger, A.; Puget, J. L. *Astron. Astrophys.* **1984**, *137*, L5.
(2) Allamandola, L. J.; Tielens, A. G. G. M.; Barker, J. R. *Astrophys. J.* **1985**, *290*, L25.
(3) (a) Russel, R.; Soifer, B.; Willner, W. *Astrophys. J.* **1977**, *217*, L149; (b) Russel, R.; Soifer, B.; Willner, W. *Astrophys. J.* **1978,** *220*, 568.
(4) Leger, A.; d'Hendecourt, L. *Astron. Astrophys.* **1985**, *146*, 81.
(5) van der Zwet, G. P.; Allamandola, L. J. *Astron. Astrophys.* **1985**, *146*, 76.
(6) Omont, A. *Astron. Astrophys.* **1986**, *164*, 159.
(7) Tielens, A. G. G. M.; Allamandola, L. J.; Barker, J. R.; Cohen, M. in *Polycyclic Aromatic Hydrocarbons and Astrophysics*, Leger, A., d'Hendecourt, L., Boccarra, N., Ed.; Dordrecht: Reidel, 1987; p 273.
(8) Allamandola, L. J.; Tielens, A. G. G. M.; Barker, J. R. *Astrophys. J. Suppl.* **1989**, *71*, 733.
(9) Geballe, T. R.; Tielens, A. G. G. M.; Allamandola, L. J.; Moorhouse, A.; Brand, P. W. *Astrophys. J.* **1989**, *341*, 278.
(10) Leger, A.; Boissel, P.; Desert, F. X.; d'Hendecourt, L. J. *Astron. Astrophys.* **1989**, *213*, 351.
(11) Leger, A.; d'Hendecourt, L. J.; Defourneau, D. *Astron. Astrophys.* **1989**, *216*, 148.
(12) Verstraete, L.; Leger, A.; d'Hendecourt, L. J.; Dutuit, O.; Defourneau, D. *Astron. Astrophys.* **1990**, *237*, 436.
(13) Allamandola, L. J.; Hudgins, D. M.; Sandford, S. A. *Astrophys. J.* **1999**, *511*, L125.
(14) Jochims, H. W.; Baumgärtel, H.; Leach, S. *Astrophys. J.* **1999**, *512*, 500.
(15) Snow, T. P.; Witt, A. N. *Science* **1995**, *270*, 1455.
(16) Pachuta, S. J.; Kenttämaa, J. I.; Sack, T. M.; Cerny, R. L.; Tomer, K. B.; Gross, M. L.; Pachuta, R. R.; Cooks, R. G. *J. Am. Chem. Soc.* **1988**, *110*, 657.
(17) Léger, A.; Boissel, P.; Désert, F. X.; d'Hendecourt, L. *Astron. Astrophys.* **1989**, *213*, 351.
(18) Boissel, P.; Lefèvre, G.; Thiébot, Ph. in *Conference Proceedings No. 312 Molecules and Grains in Space*; Nenner, I., Ed.; American Institute of Physics: New York, 1994; p 667.
(19) Boissel, P.; de Parseval, P.; Marty, P.; Lefèvre, G.; *J. Chem. Phys.* **1997**, *106*, 4973.
(20) Allain, T.; Leach, S.; Sedlmayr, E. *Astron. Astrophys.* **1996**, *305*, 602, 616.
(21) Jochims, H. W.; Rasekh, J.; Rühl, E.; Baumgärtel, H.; Leach, S. *Chem. Phys.* **1992**, *168*, 159.
(22) Lifshitz, C. *Int. Rev. Phys. Chem.* **1997**, *16*, 113.
(23) Dunbar, R. D. *Mass Spectrom. Rev.* **1992**, *11*, 309.
(24) Ho, Y.; Yang, Y.; Klippenstein, S. J.; Dunbar, R. C. *J. Phys. Chem.* **1995**, *99*, 12115.
(25) Gauthier, J. W.; Trautman, D. B.; Jacobson, D. B. *Anal. Chim. Acta* **1991**, *246*, 211.
(26) Guo, X.; Sievers, H. L.; Grützmacher, H. F. *Int. J. Mass Spectrom.* **1999**, *185*, 1.
(27) Granucci, G.; Ellinger, Y.; Boissel, P. *Chem. Phys.* **1995**, *191*, 165.
(28) Ling, Y.; Martin, J. M. L.; Lifshitz, C. *J. Phys. Chem.* **1997**, *101*, 219.
(29) Schroeter, K.; Schröder, D.; Schwarz, H. *J. Phys. Chem.* **1999**, *103*, 4174.
(30) Joblin, C.; Masselon, C.; Boissel, P.; de Parseval, P.; Martinovic, S.; Muller, J. *Rapid Commun. Mass Spectrom.* **1997**, *11*, 1619.
(31) Ekern, S. P.; Marshall, A. G.; Szczepanski, J.; Vala, M. *Astrophys. J.* **1997**, *488*, L39.
(32) Ekern, S. P.; Marshall, A. G.; Szczepanski, J.; Vala, M. *J. Phys. Chem.* **1998**, *102*, 3498.
(33) (a) Yang, Y.; Linnert, H. V.; Riveros, J. M.; Williams, K. R.; Eyler, J. R. *J. Phys. Chem.* **1997**, *101*, 2371; (b) Kage, D., Ph.D. Dissertation, University of Florida, December, 1999.
(34) Senko, M. W.; Canterbury, J. D.; Guan, S.; Marshall, A. G. *Rapid Commun. Mass Spectrom.* **1996**, *10*, 1839.
(35) Marshall, A. G.; Wang, T. C. L.; Ricca, T. L. *J. Am. Chem. Soc.* **1985**, *107*, 7893.
(36) Szczepanski, J.; Pearson, W.; Dibben, M.; Eyler, J.; Vala, M., manuscript in preparation.
(37) Shida, T. *Electronic Absorption Spectra of Radical Ions*; Elsevier: Amsterdam, 1988.
(38) Richardson, D., University of Florida, private communication; http://www.chem.ufl.edu/~der/chm6621.htm.
(39) Oomens, J.; van Roji, A. J. A.; Meijer, G.; van Helden, G. *Astrophys. J.* **2000**, *542*, 404.
(40) Felker, P. M.; Zewail, A. H. J. *Chem. Phys.* **1985**, *82*, 2975.
(41) Sun, J.; Grutzmacher, H. F.; Lifshitz, C. *Intl. J. Mass Spectrom.***1994**, *138*, 49.
(42) Beck, M. E.; Rebentisch, R.; Hohlneicher, G.; Fülscher, M. P.; Serrano-Andrés, L.; Roos, B. *J Chem. Phys.* **1997**, *107*, 9464.